

Published in final edited form as:

Bioorg Med Chem Lett. 2012 October 1; 22(19): 6233–6236. doi:10.1016/j.bmcl.2012.08.010.

Synthesis, radiolabeling and initial in vivo evaluation of [¹¹C]KSM-01 for imaging PPAR-α receptors

Kiran Kumar Solingapuram Sai^a, Kun-eek Kil, Zhude Tu^a, Wenhua Chu^a, Brian N. Finck^b, Justin M. Rothfuss^a, Kooresh I. Shoghi^a, Michael J. Welch^a, Robert J. Gropler^a, and Robert H. Mach^{a,*}

^aDivision of Radiological Sciences, Washington University School of Medicine, 510 S Kingshighway Blvd, St. Louis, MO 63110 USA

^bDivision of Geriatrics and Nutritional Science, Washington University School of Medicine, 660 S. Euclid Ave, Box 8031, St. Louis, MO 63110 USA

Abstract

Peroxisome proliferator-activated receptor alpha (PPAR-α) is a ligand-activated nuclear receptor transcription factor that regulates the fatty acid β-oxidation. An in vitro assay identified the *p*-methoxy phenyl ureido thiobutyric acid derivative **KSM-01** (IC₅₀=0.28±0.09 nM) having a higher affinity to activate PPAR-α than the PPAR-α agonist **GW7647** (IC₅₀=0.46±0.19 nM). In this study, we report the synthesis and initial in vivo evaluation of [¹¹C]**KSM-01**. The radiosynthesis was carried out by first alkylating the corresponding *p*-phenol precursor with [¹¹C]MeI in DMF using NaOH, followed by deprotection of the *t*-butyl ester group by TFA, yielding [¹¹C]**KSM-01**. SUV analysis of dynamic micro PET/CT imaging data showed that [¹¹C]**KSM-01** accumulation was ~2.0-fold greater in cardiac-specific PPAR-α overexpressing transgenic mice compared to wild-type littermates. The post-PET biodistribution studies were consistent with these results and demonstrated 2.5-fold greater radiotracer uptake in the heart of transgenic mice compared to the wild-type littermates. These results demonstrate the potential utility of PPAR-α agonists as PET radiopharmaceuticals.

Keywords

peroxisome proliferator-activated receptor alpha; (PPAR-α); β-oxidation; PET imaging; Cardiomyopathy; Ureido thioisobutyric acid (TiBA)

Peroxisome proliferator activated receptors (PPAR) are ligand-activated transcription factors which belong to the nuclear receptor gene family.^{1–3} PPARs bind to endogenous ligands including eicosanoids, free fatty acids, leukotrienes, and prostaglandins and are classified into three subtypes: PPAR-α, PPAR-β/δ and PPAR-γ.^{1, 3} Ligand-activated PPARs bind to

© 2012 Elsevier Ltd. All rights reserved.

Corresponding author: Tel.: +1 314-362-8538; fax: +1 314-362-0039; rhmach@mir.wustl.edu.
Michael J. Welch (deceased)

Publisher's Disclaimer: This is a PDF file of an unedited manuscript that has been accepted for publication. As a service to our customers we are providing this early version of the manuscript. The manuscript will undergo copyediting, typesetting, and review of the resulting proof before it is published in its final citable form. Please note that during the production process errors may be discovered which could affect the content, and all legal disclaimers that apply to the journal pertain.

Supplementary Material

Supplementary material associated with this article (chemistry, radiochemistry, QC, in vitro assay, and in vivo experimental procedures) can be found in the online Supplemental Methods at

the retinoid X receptor (RXR) to form heterodimer complexes that trigger PPAR-response elements (PPRE) which modulate lipid, glucose, or cholesterol associated metabolic pathways, depending on the nature of ligand.^{3, 4} PPAR- α plays a vital role in regulating cellular fatty acid β -oxidation and ketogenesis and is activated by a wide range of fibrate drugs; this activation induces proliferation of peroxisomes. PPAR- α is highly expressed in tissues with significant breakdown of fatty acids including liver, heart, brown adipose tissue, kidney and intestine.⁵⁻⁸ Due to its critical role in lipid metabolism, drugs which can modulate PPAR- α are being evaluated as targeted therapeutic strategies against cardiovascular diseases including type 2 diabetes mellitus, lipodistropy, and atherosclerosis.⁹

PPAR- α agonists have been studied extensively as therapeutic candidates for atherosclerosis because they down-regulate production of the adhesion molecule VCAM-1, which is responsible for endothelial cell activation in the arterial wall during atherosclerotic disease progression.^{10, 11} PPAR- α agonists may be involved in prevention of HDL cholesterol accumulation especially in cardiocytes and could affect the body weight by regulating fatty acid oxidation, thus also playing a potentially important role in diabetic cardiomyopathy.^{11, 12} Hypolipidemic fibrate drugs are an important class of PPAR- α ligands; however, fibrates which are considered highly selective *in vivo* activators of hepatic PPAR- α in rodents, often do not express the same level of selectivity in humans; many are also only moderately selective for PPAR- α over the PPAR- γ and PPAR- δ subtypes.³ Attempts to identify more potent PPAR- α ligands have led to synthesis of ureidofibrates that are active at lower concentrations in rodent models of hyperlipidemia. The ureido thioisobutyric acid (TiBA) derivative **GW9578** was observed to be a more potent and selective PPAR- α agonist with lipid-lowering activity when compared to traditional fenofibrate derivatives.¹³ However, difficulties in handling **GW9578**, which is a viscous oil, and its poor selectivity for human PPAR- α led to development of **GW7647**, which demonstrated ~200 fold selectivity towards human PPAR- α over PPAR- γ and PPAR- δ .¹⁴ Considerable literature evidence suggests that sufficient PPAR- α density exists in cardiac cells for the evaluation of agonists in imaging studies.^{10, 12} Transgenic mice with cardiac-specific overexpression of PPAR- α display a phenotype similar to that of human diabetic cardiomyopathy. Furthermore, several diabetic metabolic abnormalities, including higher fatty acid and lower glucose uptake were observed in a transgenic mouse model with cardiac-specific overexpression of PPAR- α .^{10, 12, 15}

Previous attempts have been made to measure PPAR- α activity using PPRE luciferase transgenic mice through *in vivo* and *ex vivo* bioluminescence imaging.¹⁶ However, to date, no PET tracer has been reported for the *in vivo* imaging of PPAR- α in the heart. A PPAR- α agonist as a PET radiotracer would thus become a pivotal tool to fill critical gaps in understanding the pathogenesis of diabetic cardiomyopathy triggered by PPAR- α . The ureido-TiBA derivative **GW7647** (Figure 1) has been investigated as potent PPAR- α agonist in connection with metabolic syndromes like dyslipidemia and atherosclerosis.¹⁴

GW7647 was used as a lead in designing a PET tracer by replacing the cyclohexyl group with a methoxyphenyl group; we synthesized the -2, -3, and -4 methoxyphenyl isomers of *tert*-butyl-2-(4-(2-(1-(4-cyclohexylbutyl)-3-methoxyphenyl)ureido)ethyl)phenylthio)-2-methylpropanoate as potential PPAR- α radiotracers. The structure activity relationships derived through *in vitro* binding assay results indicated the *p*-methoxyphenyl ureidothiobutyric derivative **KSM-01** (Figure 1) $IC_{50}=0.28\pm 0.09$ nM had the highest affinity to activate PPAR- α among the -*o*-, -*m*-, -*p* methoxyphenyl isomers. This report describes the synthesis, radiolabeling and initial *in vivo* microPET evaluation of [¹¹C]**KSM-01** to image PPAR- α in cardiac-specific PPAR- α overexpressing mice.

The syntheses of **KSM-01**, **02**, **03** are shown in Scheme 1 and described in detail in the online Supplemental Methods. Reduction of 4-mercaptobenzoic acid **1** with LiAlH₄ in THF resulted in the primary alcohol **2**.¹⁷ The sulfur group on **2** was alkylated with α -bromoisobutyrate in KOH-EtOH¹³ to give compound **3** after which the hydroxyl group in **3** was converted to the corresponding chloro analog **4** using PPh₃ in CCl₄.¹⁸ Cyanation and reductive amination of compound **4** using KCN and BH₃.THF respectively gave the amine analog **5**.¹⁹ Further reaction with 4-cyclohexyl-1-bromobutane²⁰ in DIPEA and THF gave the secondary amine **6**,²¹ which was coupled with 2-methoxy, 3-methoxy, or 4-methoxy phenylisocyanate followed by TFA-assisted *t*-butyl ester deprotection to give analogs **KSM-03**, **KSM-02** and **KSM-01** respectively.¹³ The precursor **KSM-01A** for ¹¹C-radiolabeling was obtained from the secondary amine **6** coupled with 1,1'-dicarbonyl imidazole followed by 4-amino phenol in THF.¹³

PPAR- α binding affinity of **KSM-01**, **KSM-02** and **KSM-03** was assessed to identify the most potent PPAR- α agonist. Using a beta-lactamase reporter-gene under control of the PPAR- α response element, a cell-based assay developed by Invitrogen was used to determine the IC₅₀ values of the novel PPAR- α ligands. Novel PPAR- α compounds were measured for their ability to inhibit reporter gene activity. The assay utilizing GeneBLAzer PPAR- α UAS-*bla* HEK293T cells is described in detail in the online Supplemental Methods. The fluorescence intensity was measured using a Victor³ plate reader after addition of the LiveBLAzer™-FRET B/G (CCF4-AM) substrate. Concentration-response titration points for each compound were fitted to the Hill equation yielding concentrations of halfmaximal inhibition (IC₅₀) and maximal response (efficacy) values. The IC₅₀ values of the analogs are shown in Table 1.^{16, 21} Compound **KSM-01** showed higher potency towards PPAR- α compared to the two isomers and the previously reported PPAR- α agonist **GW7647**, suggesting that **KSM-01** could be a suitable PPAR- α PET imaging agent.

The radiochemical synthesis of [¹¹C]**KSM-01** is described in detail in the online Supplemental Methods. It was achieved by first alkylating the corresponding *p*-phenol precursor **KSM-01A** with [¹¹C]MeI in DMF using NaOH at 90°C for 5 min and then deprotecting the *t*-butyl ester group with trifluoroacetic acid at 90°C for 3 min as depicted in Scheme 2. The total time required for the synthesis of [¹¹C]**KSM-01**, including [¹¹C]MeI production, purification and formulation was approximately 50 min. The radiochemical purity of [¹¹C]**KSM-01** was >98% and was confirmed by co-elution with non-radioactive **KSM-01**. The chemical purity of [¹¹C]**KSM-01** determined by the HPLC UV mass was >97%. The calculated radiochemical yield was ~19% and the final product had a specific activity of 987 mCi/ μ mol (decay-corrected to end of synthesis).

The uptake of [¹¹C]**KSM-01** was compared in transgenic mice with cardiac-specific overexpression of PPAR- α (PPAR- α +/+) and wild type littermates (PPAR- α -/-) through microPET imaging and post-PET biodistribution studies as described in the online Supplemental Methods. Transgenic mice were produced as previously described.¹⁰ PPAR- α protein levels are approximately 15-fold more abundant in the cardiac ventricles of these transgenic animals when compared with wildtype littermates; this model has been used to evaluate the role of PPAR- α mediated lipid metabolism in the development of diabetic cardiomyopathy.¹⁰

Dynamic PET imaging was performed for 0–60 min post intravenous injection of [¹¹C]**KSM-01**. Standard uptake values (SUVs) analysis of the PET data revealed a 2-fold greater accumulation of radioactivity in PPAR- α overexpressing transgenic mice (0.68 \pm 0.007) over the control animals (0.37 \pm 0.09). Although liver uptake is significant, microPET images show higher [¹¹C]**KSM-01** accumulation in the heart of PPAR- α overexpressing transgenic mice compared to wild-type mice (Figure 2).

A post-PET biodistribution study was also conducted and the results are presented in Table 2. Radiotracer accumulation was observed to be high in liver tissue, which is a primary organ for PPAR- α expression⁵⁻⁸ in both transgenic and control animals: %ID/g = 55.031 \pm 4.926 and 60.699 \pm 0.774 respectively. Additionally, the radiotracer demonstrated ~2.5 fold greater distribution in the cardiac tissue of PPAR- α overexpressing transgenic mice (1.09 \pm 0.246) when compared to the wild type littermates (0.479 \pm 0.007) (Figure 3). The biodistribution results were consistent with the microPET imaging data.

In summary, the ureido TiBAC analog **KSM-01**, a PPAR- α agonist with high potency (IC₅₀ = 0.28 nM) was synthesized and [¹¹C]-radiolabeled for the first time. MicroPET imaging data comparing transgenic mice which selectively overexpress PPAR- α in the heart with wild-type littermates indicate the potential utility of PPAR- α agonists as PET radiopharmaceuticals. Although liver uptake is high due to the normal expression of PPAR- α , elevated cardiac uptake can be clearly visualized in PPAR- α over-expressing transgenic mice. Further experiments evaluating this strategy with ¹⁸F-radiolabeled PPAR- α agonists are currently underway.

Supplementary Material

Refer to Web version on PubMed Central for supplementary material.

Acknowledgments

The authors thank Washington University School of Medicine Cyclotron Facilities for carbon-11 methyl iodide production and the Small Animal Imaging Core for conducting the rodent studies. This research was funded by HL13851.

References

1. Berger J, Moller DE. *Annu. Rev. Med.* 2002; 53:409. [PubMed: 11818483]
2. Berger JP, Akiyama TE, Meinke PT. *Trends Pharmacol. Sci.* 2005; 26:244. [PubMed: 15860371]
3. Willson TM, Brown PJ, Sternbach DD, Henke BR. *J. Med. Chem.* 2000; 43:527. [PubMed: 10691680]
4. Nolte RT, Wisely GB, Westin S, Cobb JE, Lambert MH, Kurokawa R, Rosenfeld MG, Willson TM, Glass CK, Milburn MV. *Nature.* 1998; 395:137. [PubMed: 9744270]
5. Bolignano D, Zoccali C. *Nutr. Metab. Cardiovas.* 2012; 22:167.
6. Holden P, Tugwood J. *J. Mol. Endocrinol.* 1999; 22:1. [PubMed: 9924174]
7. Kliewer SA, Umesono K, Noonan DJ, Heyman RA, Evans RM. *Nature.* 1992; 358:771. [PubMed: 1324435]
8. Michalik L, Auwerx J, Berger JP, Chatterjee VK, Glass CK, Gonzalez FJ, Grimaldi PA, Kadowaki T, Lazar MA, O'Rahilly S, Palmer CN, Plutzky J, Reddy JK, Spiegelman BM, Staels B, Wahli W. *Pharmacol. Rev.* 2006; 58:726. [PubMed: 17132851]
9. Zheng Z, Yang Y, Shao H, Liu Z, Lu X, Xu Y, He X, Jiang W, Jiang Q, Zhao B, Zhang H, Li Z, Si S. *Biol. Phar. Bull.* 2011; 34:1631.
10. Finck BN, Han X, Courtois M, Aimond F, Nerbonne JM, Kovacs A, Gross RW, Kelly DP. *Proc. Natl. Acad. Sci. U.S.A.* 2003; 100:1226. [PubMed: 12552126]
11. Issemann I, Green S. *Nature.* 1990; 347:645. [PubMed: 2129546]
12. Barger PM, Kelly DP. *Trends. Cardiovasc. Med.* 2000; 10:238. [PubMed: 11282301]
13. Brown PJ, Winegar DA, Plunket KD, Moore LB, Lewis MC, Wilson JG, Sundseth SS, Koble CS, Wu Z, Chapman JM, Lehmann JM, Kliewer SA, Willson TM. *J. Med. Chem.* 1999; 42:3785. [PubMed: 10508427]
14. Brown PJ, Stuart LW, Hurley KP, Lewis MC, Winegar DA, Wilson JG, Wilkison WO, Ittoop OR, Willson TM. *Bioorg. Med. Chem. Lett.* 2001; 11:1225. [PubMed: 11354382]

15. Finck BN, Lehman JJ, Leone TC, Welch MJ, Bennett MJ, Kovacs A, Han X, Gross RW, Kozak R, Lopaschuk GD, Kelly DP. *J. Clin. Invest.* 2002; 109:121. [PubMed: 11781357]
16. Biserni A, Giannesi F, Sciarroni AF, Milazzo FM, Maggi A, Ciana P. *Mol. Pharmacol.* 2008; 73:1434. [PubMed: 18292206]
17. DeCollo TV, Lees WJ. *J. Org. Chem.* 2001; 66:4244. [PubMed: 11397160]
18. Barfoot CW, Harvey JE, Kenworthy MN, Kilburn JP, Ahmed M, Taylor RJK. *Tetrahedron.* 2005; 61:3403.
19. David E, Rangheard C, Pellet-Rostaing S, Lemaire M. *Synlett.* 2006; 2006:2016.
20. Blecha JE, Anderson MO, Chow JM, Guevarra CC, Pender C, Penaranda C, Zavodovskaya M, Youngren JF, Berkman CE. *Bioorg. Med. Chem. Lett.* 2007; 17:4026. [PubMed: 17502145]
21. Heerding DA, Rhodes N, Leber JD, Clark TJ, Keenan RM, Lafrance LV, Li M, Safonov IG, Takata DT, Venslavsky JW, Yamashita DS, Choudhry AE, Copeland RA, Lai Z, Schaber MD, Tummino PJ, Strum SL, Wood ER, Duckett DR, Eberwein D, Knick VB, Lansing TJ, McConnell RT, Zhang S, Minthorn EA, Concha NO, Warren GL, Kumar R. *J. Med. Chem.* 2008; 51:5663. [PubMed: 18800763]

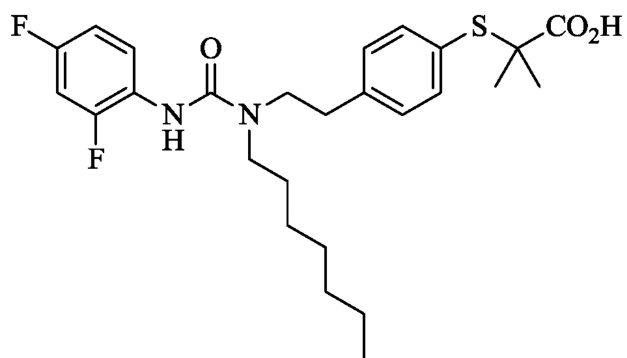
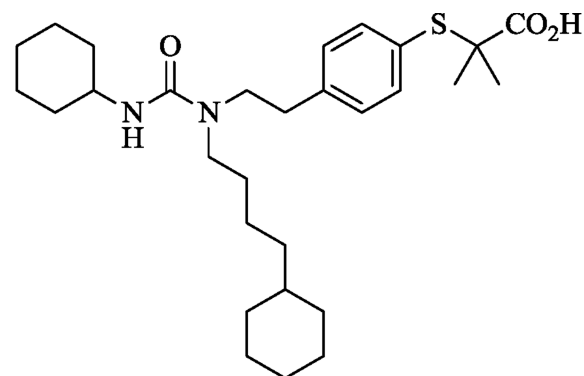
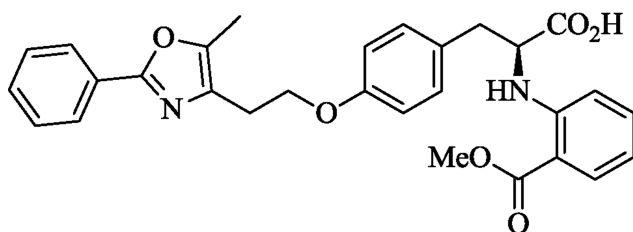
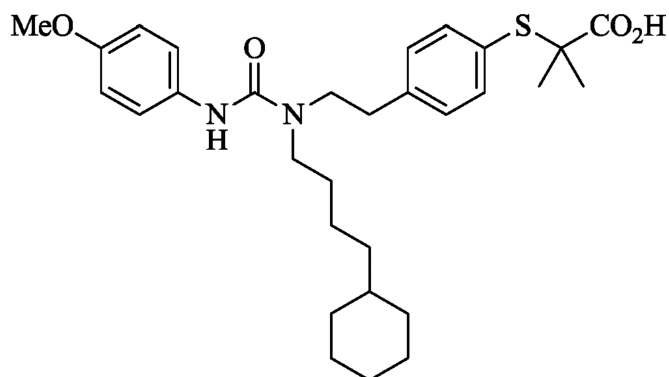
**GW9578****GW7647****GW7845****KSM-01**

Figure 1.
Structures of the ureido-TiBA PPAR-α agonists

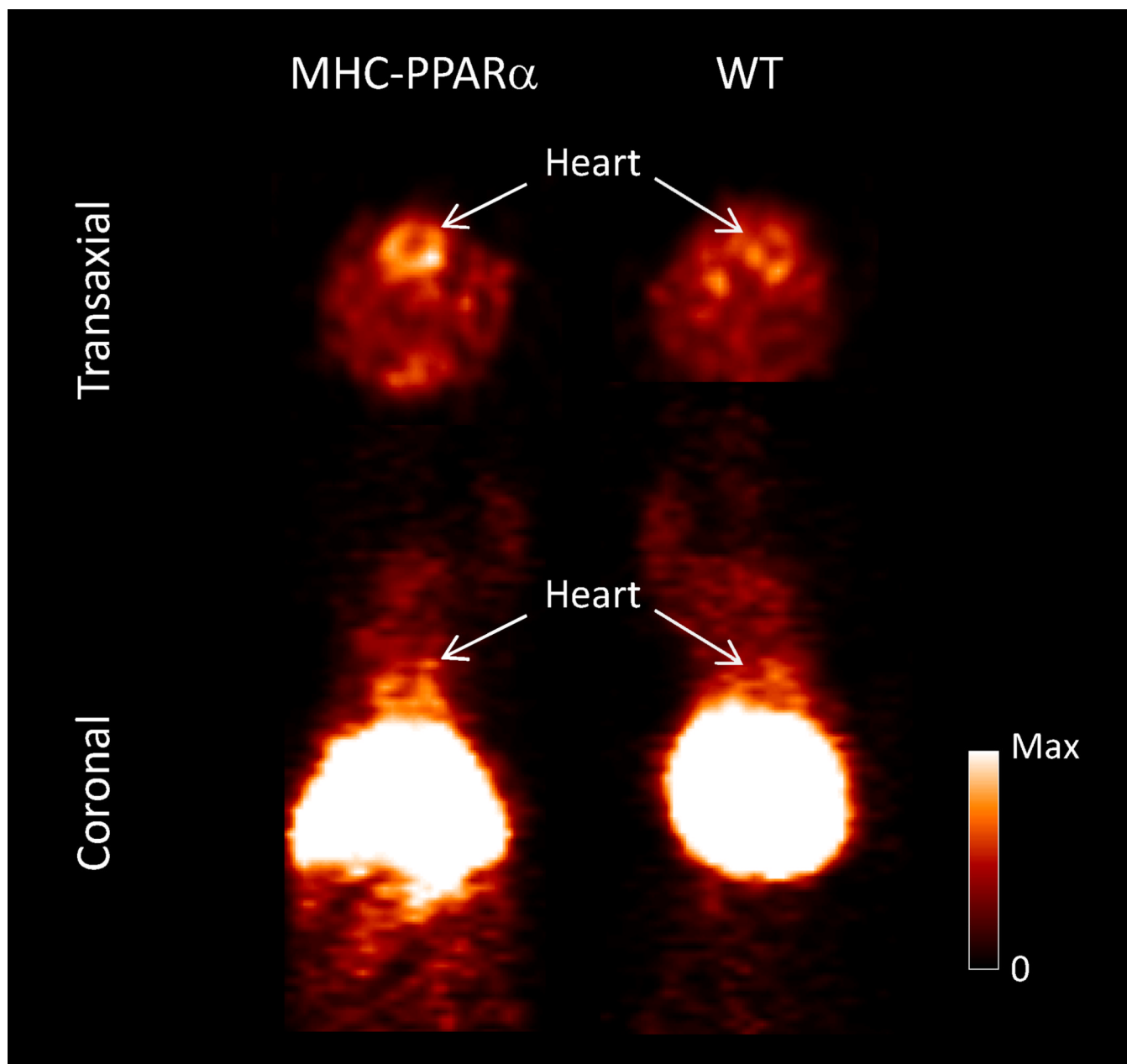


Figure 2. Representative Focus 220 microPET image of [^{11}C]KSM-01 in male MHC-PPAR- α transgenic and wild type (WT) mice. The images were summed from 0–60 min after *iv* injection of 170 μCi [^{11}C]KSM-01.

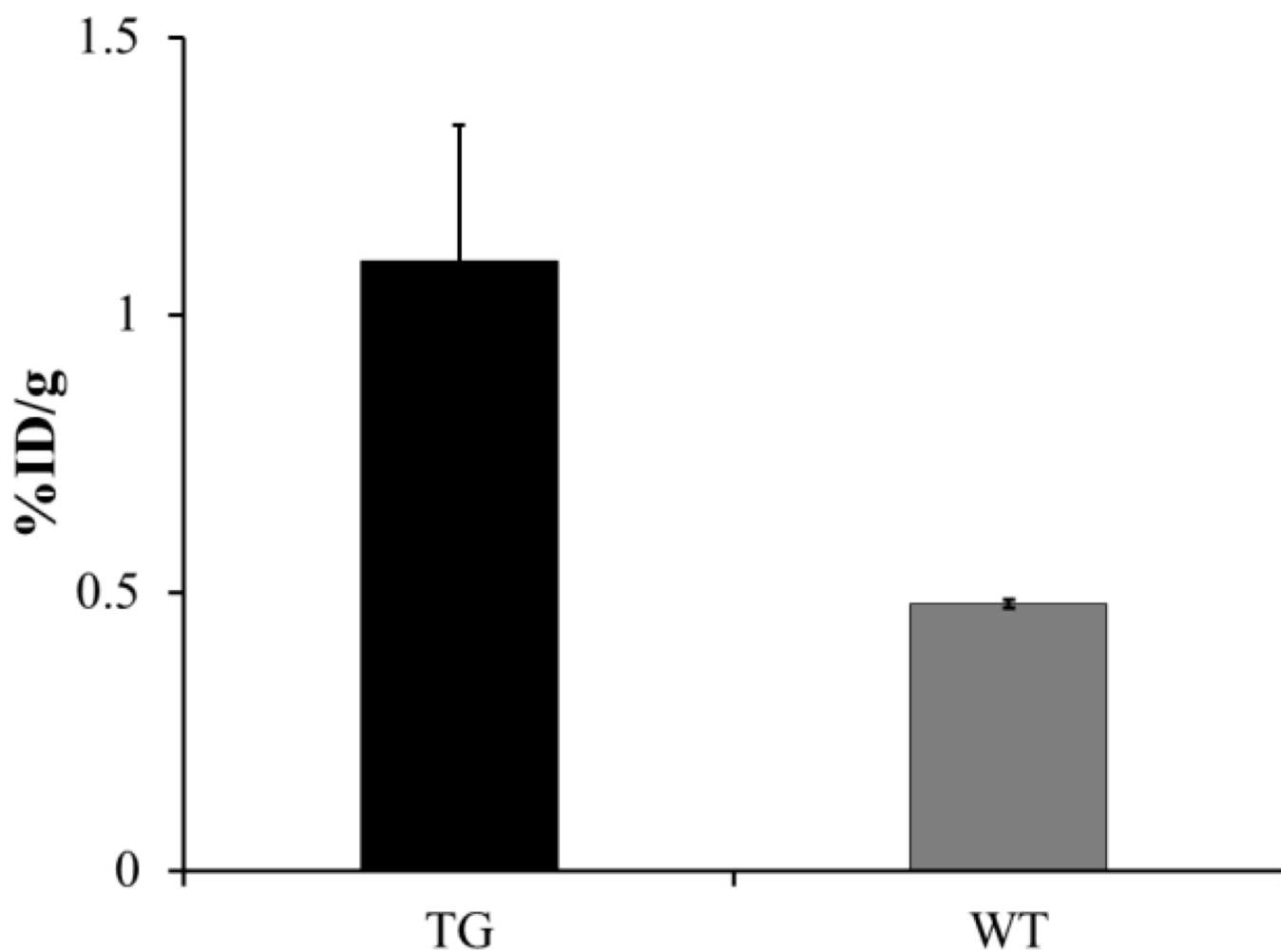
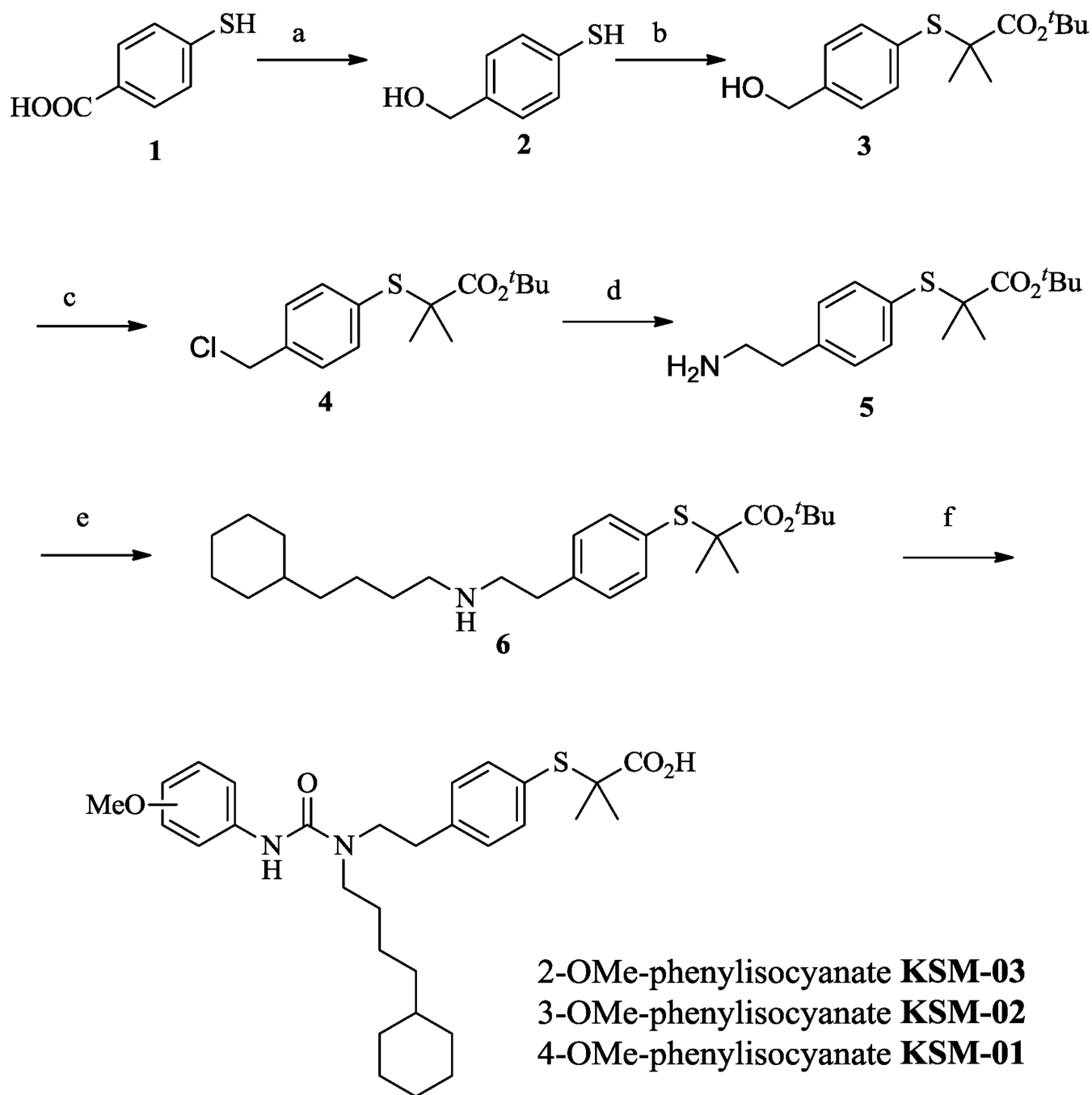
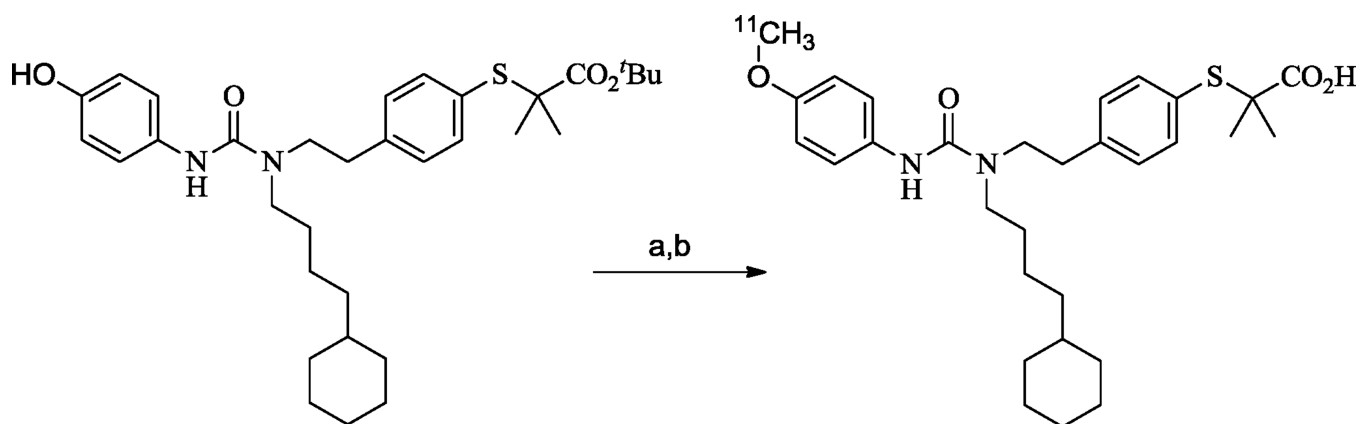


Figure 3. Post-PET uptake of $[^{11}\text{C}]\text{KSM-01}$ in cardiac tissue (%ID/g) of male MHC-PPAR- α transgenic (TG) and wild type mice (WT).

**Scheme 1.**

Reagents: (a) LiAlH_4 , THF, 67%; (b) α -bromoisobutyrate, KOH, EtOH, 94%; (c) PPh_3 , C_2Cl_6 , 95%; (d) KCN, $\text{BH}_3 \cdot \text{THF}$, 78%; (e) 4-cyclohexyl-1-bromobutane, DIPEA, 68%; (f) 2/3/4-methoxyphenylisocyanate, TFA. Yields: **KSM-03**, 65%; **KSM-02**, 85%; **KSM-01**, 90%.

**Scheme 2.**

Reagents: (a) [^{11}C]MeI, 5N NaOH, DMF, 90°C, 5 min; (b) TFA, 90°C, 3 min.

Table 1In vitro binding affinities of ureido-TiBAs for PPAR- α

Compound	IC ₅₀ (nM)
KSM-01	0.28±0.09
KSM-02	0.59±0.22
KSM-03	1.93±0.99
GW7647	0.46±0.19

Table 2

Post-PET biodistribution of [¹¹C]KSM-01 in non-target tissues of male MHC PPAR- α overexpressing transgenic (TG) and wild type mice (WT). Results are expressed as %ID/g \pm standard deviation.

Organ	TG	WT
Blood	0.42 \pm 0.14	0.42 \pm 0.10
Lung	2.65 \pm 0.34	2.11 \pm 0.31
Liver	55.30 \pm 4.92	60.69 \pm 0.77
Spleen	1.33 \pm 0.29	1.55 \pm 0.14
Kidney	2.58 \pm 0.56	2.01 \pm 0.21
Muscle	0.36 \pm 0.15	0.35 \pm 0.18